Electrical Power and Energy Systems 170 (2025) 110880

Contents lists available at ScienceDirect

International Journal of Electrical Power and Energy Systems

journal homepage: www.elsevier.com/locate/ijepes

Stochastic co-optimisation of energy, frequency and carbon services considering flexible nuclear power plants

Aimon Mirza Baig [a], Yi Wang [a,*], Marko Aunedi [b], Goran Strbac [a]

[a] Department of Electrical and Electronic Engineering, Imperial College London, London SW7 2AZ, UK
[b] Department of Electronic and Electrical Engineering, Brunel University London, London UB8 3PH, UK

ARTICLE INFO

Keywords:
Ancillary services
Renewable energy sources
Flexible nuclear power plant
Stochastic unit commitment
Operational flexibility

ABSTRACT

Integration of high levels of non-synchronous Renewable Energy Sources (RES) and nuclear power plant will play a vital role in decarbonising the electricity grid of Great Britain (GB). However, the uncertainties associated with RES may increase the risk of grid frequency deterioration, which will increase the requirement for the provision of ancillary services such as inertia and Frequency Response (FR). Furthermore, nuclear power plants typically have lower operational flexibility due to limited load following capabilities and the ability to provide FR services, which will not only lead to high system operation cost but also present a potential barrier to reach the net-zero emissions target cost-effectively by reducing the utilisation of RES. A potential solution to mitigate these challenges consists of incorporating thermal energy storage and secondary steam rankine cycle into the nuclear power plant, effectively resulting in a Flexible Nuclear Power Plant (FNPP) configuration. Therefore, this paper proposes a novel ancillary services constrained stochastic unit commitment model, which optimises the simultaneous provision of energy production, synchronised inertia and primary FR from conventional power plants and FNPP, enhanced FR from wind, whilst explicitly considering the uncertainties associated with wind generation using the quantile-based scenario tree method. The effectiveness of the proposed model is demonstrated through several case studies conducted on the 2030 GB power system. The results explore the economic savings and carbon emissions cost reductions obtained from simultaneous co-optimisation of FNPP and the provision of FR services provided by FNPP and wind.

1. Introduction

Increasing deployment of non-synchronous Renewable Energy Sources (RES) and nuclear power plants represent some of the key measures to achieve the net-zero carbon emissions target globally. To achieve the net-zero target by 2050, Great Britain (GB) is considering substantial investments not only in RES but also in increasing its nuclear power capacity [1]. In addition to supporting the delivery of the net-zero target, nuclear power is also expected to play a vital role in providing secure and reliable low-carbon electricity in the presence of high shares of variable RES [2].

Although the increasing integration of RES and nuclear power plants plays a key role in achieving net-zero emissions, it also introduces significant techno-economic challenges [3]. Technical challenges arising from the increasing integration of RES are primarily linked to their variable nature and the absence of inherent inertia. This poses a significant issue in maintaining the stability of the power grid frequency around its nominal value, especially during events involving a sudden and major loss of generation within the system [4]. The economic aspect of the challenge arises due to the technical characteristics of nuclear power plants, typically characterised by limited load following capabilities (such as e.g. ramp limits etc.) as well as a lack of ability to provide Frequency Response (FR) services due to its inflexible nature [5]. Therefore, it is of great interest to explore the flexibility that nuclear power plants can potentially provide through enhancing their load following capabilities, as well as the provision of FR services to enhance the utilisation of RES and provide frequency security in the presence of high shares of RES [6].

To provide solutions that address the said challenges, there has been an increasing interest in obtaining frequency security services such as inertia and FR, also collectively referred to as Ancillary Services (AS), from various flexible technologies such as Battery Energy Storage Systems (BESS) [7,8] and hydrogen [9] in order to maintain system stability. Research in [10] proposes a frequency-security constrained Stochastic Unit Commitment (SUC) model that simultaneously co-optimises the provision of synchronised and synthetic inertia from

* Corresponding author.
E-mail address: yi.wang18@imperial.ac.uk (Y. Wang).

https://doi.org/10.1016/j.ijepes.2025.110880
Received 19 February 2025; Received in revised form 18 June 2025; Accepted 5 July 2025
Available online 26 July 2025

Nomenclature

Indices and Sets

$i \in \mathcal{I}$	Index, Set of inverter-based sources
$t \in \mathcal{T}$	Index, Set of time
$g \in \mathcal{G}$	Index, Set of conventional power plants
$f \in \mathcal{F}$	Index, Set of flexible nuclear power plants
$n \in \mathcal{N}$	Index, Set of nodes in scenario tree
$s \in \mathcal{S}$	Index, Set of storage units

Constants and Parameters

$\pi(n)$	Probability of reaching node n in the SUC
$\Delta\tau(n)$	Time interval corresponding to node n in the SUC (h)
Δf_{max}	Maximum admissible frequency deviation at nadir (Hz)
$RoCoF_{max}$	Maximum admissible RoCoF (Hz/s)
f_o	Nominal frequency of the electricity grid (Hz)
T_{EFR}	Deliver time of EFR (s)
T_{PFR}	Deliver time of PFR (s)
H_L	Inertia constant of largest loss (s)
P_L^{max}	Upper bound for the largest loss (MW)
H_g	Inertia constant of conventional power plants (s)
C_g^{nl}	No-load cost of conventional power plants (£/h)
C_g^{m}	Marginal cost of conventional power plants (£/MWh)
C_g^{s}	Start-up cost of conventional power plants (£/h)
P_g^{msg}	Minimum power limit of conventional power plants (MW)
P_g^{max}	Maximum power limit of conventional power plants (MW)
R_g^U	Ramp-up limit of a conventional power plants g (MW)
R_g^D	Ramp-down limit of a conventional power plants g (MW)
R_g^{max}	PFR capacity by conventional power plants (MW)
$P_{i,t}$	Power available from wind turbines (MW)
P_i^{max}	Rated power of wind turbines (MW)
R_i^{max}	EFR capacity from wind turbines (MW)
D_t	Net demand at time t (MW)
P_{psrc}^{min}	Minimum power limit of PSRC (MW_{el})
P_{psrc}^{max}	Maximum power limit of PSRC (MW_{el})
P_{ssrc}^{min}	Minimum power limit of SSRC (MW_{el})
P_{ssrc}^{max}	Maximum power limit of SSRC (MW_{el})
$nlhr_{psrc}$	No-load heat rate of PSRC (MWh_{th}/h)
vhr_{psrc}	Variable heat rate of PSRC (MW_{th}/MW_{el})
$nlhr_{ssrc}$	No-load heat rate of SSRC (MWh_{th}/h)
vhr_{ssrc}	Variable heat rate of SSRC (MW_{th}/MW_{el})
H_n	Inertia constant of FNPP (s)
R_{psrc}^{max}	EFR capacity by PSRC (MW_{el})
R_{ssrc}^{max}	EFR capacity by SSRC (MW_{el})
P_{tes}^{max}	Maximum installed capacity of TES (MWh_{th})
$h_{tes,t}^{c}$	Charge rate of TES (MW_{th})
$h_{tes,t}^{d}$	Discharge rate of TES (MW_{th})
h_{sg}^{max}	Maximum heat output from SG (MW_{th})
h_{sg}^{min}	Minimum heat output from SG (MW_{th})
$P_{s,t}^{cmax}$	Maximum charging power of storage unit (MW)
$P_{s,t}^{dmax}$	Maximum discharging power of storage unit (MW)
E_s^{min}	Minimum rate of storage unit (MW)
E_s^{max}	Maximum rate of storage unit (MW)

Decision Variables

$P_{g,t}$	Power generation by conventional power plants (MW)
n_g^{sg}	Number of conventional power plants that have started generating
n_g^{up}	Number of conventional power plants that are online
$R_{g,t}$	PFR provision from conventional power plants (MW)
$R_{i,t}$	EFR provision from wind turbines (MW)
$P_{i,t}^{curt}$	Wind curtailment (MW)
P^{LS}	Total amount of load shed (MW)
P_L	Largest power infeed (MW)
$P_{psrc,t}$	Power generation by PSRC (MW_{el})
$P_{ssrc,t}$	Power generation by SSRC (MW_{el})
$R_{psrc,t}$	EFR provision from PSRC (MW_{el})
$R_{ssrc,t}$	EFR provision from SSRC (MW_{el})
$P_{s,t}^{c}$	Charging power of storage unit (MW)
$P_{s,t}^{d}$	Discharging power of storage unit (MW)
$E_{s,t}$	Energy content of storage unit (MW)
$R_{s,t}$	EFR provision from storage unit (MW)

Linear Expressions

H_t	System inertia (MW.s)
C_g	Operating cost of conventional power plants (£)
C_e	Emissions cost of conventional power plants (£)
PFR_t	Total PFR provision from all conventional power plants and FNPP (MW)
EFR_t	Total EFR provision from BESS and wind turbines (MW)
$P_{n,t}$	Power generation by flexible nuclear (MW)
C_n	Fuel cost of FNPP (£/MWh)

conventional power plants and wind respectively, FR from conventional power plants and BESS, and a dynamically reduced largest loss. Ref. [11] developed a Mixed-Integer Second-Order Cone Programming (MISOCP) model to co-optimise frequency response services from zero-carbon technologies, including inertia contributions from synchronous condensers and frequency response from curtailed renewable energy sources. Authors in [12] used a moment-based distributionally-robust chance-constrained approach to investigate the impact of Electric Vehicles (EVs) equipped with vehicle-to-grid chargers that enable them to provide FR. Another work in [13] proposed a stochastic scheduling model that allows for optimising the provision of synthetic inertia from wind turbines while ensuring system stability. However, previous studies have largely overlooked the potential contribution of nuclear power plants to providing flexibility by simultaneous co-optimisation of load following capabilities and FR provision in an optimisation

problem. Flexible Nuclear Power Plants (FNPPs) offer distinct advantages over other low-carbon flexibility technologies such as BESS and hydrogen-based systems, particularly in the provision of grid stability and AS. Unlike BESS, which are constrained by limited energy storage duration, FNPPs can sustain flexibility services over extended periods without the risk of energy depletion, making them well-suited for long-duration support during system imbalances [14]. FNPPs also contribute rotational inertia inherently due to their synchronous generation, a critical feature for frequency stability, which inverter-based technologies like BESS and hydrogen fuel cells typically lack unless supplemented with synthetic inertia [15]. Moreover, FNPPs can concurrently provide baseload electricity and frequency services—such as inertia, Primary Frequency Response (PFR), and Enhanced Frequency Response (EFR)—without significant trade-offs, while batteries must allocate limited capacity between these functions [16]. Hydrogen systems, though promising for seasonal storage, suffer from lower round-trip efficiencies and slower dynamic response times, limiting their effectiveness in real-time frequency regulation [17]. As such, integrating FNPPs into system operations presents a cost-effective and technically robust strategy to enhance flexibility, reduce emissions, and support the stable operation of high-renewable power systems.

The primary challenge lies in the mathematical complexity of co-optimising load following capabilities and the provision of flexibility and FR by nuclear power plants within the frequency security constrained optimisation framework, which is further compounded by uncertainties introduced by RES. Flexibility from nuclear power plant can be significantly enhanced by equipping them with technologies such as Thermal Energy Storage (TES) and the Secondary Steam Rankine Cycle (SSRC), resulting in a Flexible Nuclear Power Plant (FNPP) configuration. This flexible configuration could allow nuclear units to effectively contribute to the system's load following capabilities and provide FR. FR provision from FNPP can be co-optimised in the optimisation framework to provide Primary FR (PFR) service that must be fully delivered within 10 s after the contingency occurs, in contrast to the Enhanced FR (EFR) that must be fully delivered within 1 s of contingency.

In this context, several ways of co-optimising flexibility from nuclear power plants have been investigated in [18–24]. More specifically, the authors in [18] demonstrates that coupling thermal energy storage with nuclear Rankine cycles enhances baseload flexibility, increasing capacity factor by up to 9.8%. Furthermore, authors is [19] conducted an analysis to investigate the performance of nuclear power plants integrated with TES in the presence of high shares of RES. According to [20], integrating TES with nuclear power plants improves their operational flexibility and economic performance by supporting peak-load generation, enabling energy arbitrage, and providing AS, with overall profitability influenced by factors such as storage size, system configuration, and market dynamics. Another study in [21] suggested that co-optimising nuclear power plants operation with TES can enhance flexibility, be cost-effective, and reduce emissions depending on the generation mix, presence of demand-side response and regulatory structure. Ref. [22] proposed that the incorporation of cryogenic-based energy storage technology with nuclear power plants can enhance the power output by 2.7 times. Furthermore, the authors in [23] evaluated the profits that the nuclear power plant incorporated with TES and secondary generators can generate, and found that its revenue could increase by 3%–8%. Another study in [24] shows that the power output of a nuclear power plant could be increased by 24% when the stored thermal energy is discharged using a secondary Organic Rankine Cycle (ORC). All previous studies demonstrate the cost benefits of FNPP. However, none of the previous publications focused on the provision of FR services from FNPP in a frequency security constrained optimisation framework, while explicitly considering the uncertainty introduced by RES.

Furthermore, an approach to co-optimising the investment in FNPP components with investment in other energy system assets has been proposed in [25], identifying cost-efficient configurations of FNPPs that minimise total system cost in a decarbonised energy system. However, it does not explicitly account for the provision of frequency security nor consider the uncertainties introduced by RES. This gap in research highlights the need for a more integrated approach to understanding how frequency security mechanisms can enable FNPP to contribute more effectively to grid stability and carbon emission cost reduction, especially in stochastic systems with high penetration of RES.

Given the above research gaps, the present research proposes a frequency security or AS-constrained optimisation framework that considers specific constraints related to FNPP and co-optimises the provision of energy, frequency, and carbon services from various resources, including FNPPs, RES and conventional power plants, while considering uncertainties associated with RES. The main contributions of this research are outlined below:

(1) This paper proposes a novel Ancillary Services Constrained Stochastic Unit Commitment (ASCSUC) model that, for the first time, allows simultaneous co-optimisation of flexibility and FR provision from FNPP in a frequency security-constrained optimisation framework that accounts for uncertainties from RES.
(2) The proposed ASCSUC model is formulated as a Mixed-Integer Linear Program (MILP), and incorporates the constraints for various components (including SSRC and TES) of the FNPP, while allowing simultaneous scheduling of energy production, provision of PFR from conventional power plants and FNPP, and EFR from wind turbines.
(3) The proposed formulation explicitly considers the uncertainty of wind generation using a quantile-based scenario tree method. The building of scenario trees for each time step is repeated for the entire duration of the simulations in a rolling planning approach.
(4) Comprehensive case studies have been conducted to evaluate the accuracy and computational efficiency of simultaneous co-optimisation of FNPPs and AS contributions from FNPP and wind, in providing system stability within the scenario of the future GB power system. In addition to providing system stability, the analysis demonstrates that the GB 2030 power system will benefit significantly from the increase of AS contribution from FNPP and wind in reaching the net-zero emission target.

The remainder of this paper is organised as follows: Section 2 details the configuration for the FNPP and describes the fundamentals of frequency security requirements in power systems. Section 3 presents the mathematical formulation of the optimisation problem. Section 4 illustrates the applicability of the proposed model through several case studies. Finally, the conclusions are drawn in Section 5.

2. Flexible nuclear power plant and requirements for frequency security

This section discusses the layout and characteristics of the FNPP, followed by the system dynamics associated with frequency security requirements to ensure system stability in the event of a major supply loss.

2.1. Flexible nuclear power plant configuration

A nuclear power plant largely operates like a conventional power plants that generates electricity from heat [26]. However, the technical characteristics of conventional power plants generally allow them to provide load-following capabilities such as ramping up or down, or starting up and shutting down when required. On the other hand, nuclear power plants, which typically consist of a nuclear reactor, steam generator and a Steam Rankine Cycle generator, are generally not designed to be turned on or off at short notice or provide variable power output; instead, they are normally operated as baseload generation,

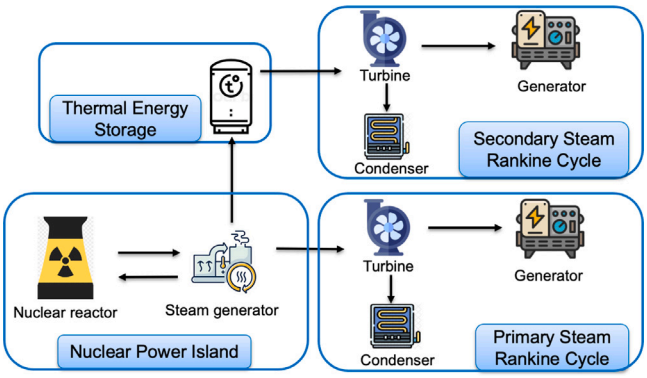

Fig. 1. The schematic for the proposed flexible nuclear power plant.

Table 1
Technical parameters for flexible nuclear power plant.

Type	Flexible Nuclear
Number of units	6
PSRC max power limit (MW_{el})	1,800
PSRC min stable generation (MW_{el})	900
SSRC max power limit (MW_{el})	520
SSRC min stable generation (MW_{el})	250
PSRC variable heat rate (MW_{th}/MW_{el})	2.65
PSRC no-load heat rate (MWh_{th}/h)	248.8
SSRC variable heat rate (MW_{th}/MW_{el})	3.81
SSRC no-load heat rate (MWh_{th}/h)	0
Max FR capacity PSRC (MW_{el})	180
Max FR capacity SSRC (MW_{el})	52
SG min output (MW_{th})	4,400
SG max output (MW_{th})	5,500
TES size (MWh_{th})	1,948
TES charge max (MW_{th})	2,164
TES discharge max (MW_{th})	1,753

i.e., at constant full power output for long periods of time (a year or even more) [27]. This subsection describes the proposed configuration of the FNPP that represents an upgraded version of the conventional nuclear power plants with enhanced load-following capability and the ability to provide flexible FR services. The main components of the FNPP are illustrated in Fig. 1 and described below:

(1) **Nuclear Power Island**: It consists of a nuclear reactor and a Steam Generator (SG). The nuclear reactor is the core of the nuclear power plant where nuclear fission is used to generate heat. The heat from the nuclear reactor is then transferred to the SG, where the water is boiled to produce steam.
(2) **Primary Steam Rankine Cycle (PSRC)**: PSRC is directly connected to the SG and consists of a turbine, condenser, and an electric generator. The steam from the SG is received by the steam turbine that transforms the heat contained in the steam into mechanical rotation. This mechanical rotation is then converted into electricity using a synchronous generator. Finally, the steam coming out of the turbine goes into the condenser, where cooling water circulates to condense the steam into water that is ready to enter the SG and continue the cycle [28].
(3) **Thermal Energy Storage (TES)**: The TES unit is connected to the SG and is charged using some of the steam flowing out of the SG. During off-peak hours when the demand is low and there is excess generation, the FNPP has the capability to reduce its power output by reducing the amount of electricity generated in the PSRC. Instead, the excess steam from the SG is utilised to charge the TES.
(4) **Secondary Steam Rankine Cycle (SSRC)**: This is the secondary power generating unit that is attached to the TES. Unlike the PSRC, which generates electricity using the steam from SG, SSRC can generate electricity by discharging the heat stored in TES, typically during peak demand hours.

In contrast to the conventional nuclear units that need to operate close to their maximum capacity to maximise their economic benefits, in this research it is assumed that during off-peak hours the FNPP has the capability to reduce its output power from 1,800 MW to 900 MW, and store excess heat from the SG in the TES unit. This stored heat energy can then be discharged to operate the SSRC during high peak demand periods, effectively increasing the total FNPP output above the capacity of the PSRC itself. Some of the key operating parameters of the FNPP are described in Table 1 below. Detailed thermodynamic parameters and an explanation of the FNPP operation can be found in [5].

2.2. Requirements for frequency security

The electric frequency of a power system must always be kept within the defined security threshold (50 Hz in the case of the GB power system) following the loss of a large generator. The three post-fault frequency security requirements that must be met by any power system as shown in Fig. 2 are [29]:

(1) Rate-of-Change-of-Frequency (RoCoF) represents the rate at which the grid's frequency changes over time. The maximum RoCoF limit is currently set by National Grid to 0.125 Hz/s. However, this limit is expected to gradually become relaxed to 0.5 Hz/s and 1 Hz/s through the Accelerated Loss of Mains Change Programme [30].
(2) Frequency Nadir represents the lowest value that the grid's frequency can attain after generator loss. To avoid the activation of Low-Frequency Demand Disconnection (LFDD), the frequency nadir must not fall below 49.2 Hz.
(3) Quasi-steady-state (q-s-s) frequency, which must recover to at least 49.5 Hz within 60 s after a generation loss event [31].

Adhering to these safe boundaries allows the system operator to meet the post-fault frequency requirements, even during unexpected generator losses [32]. To ensure system stability and meet post-fault frequency security requirements, the generation dispatch must also secure a sufficient volume of AS, such as inertia, EFR and PFR [33]. The post-fault frequency security requirements are obtained from the swing equation (2.1), which captures the fluctuations of frequency in the event of a major generation outage [34] as shown in Fig. 2:

$$\frac{2H_t}{f_0}\cdot\frac{\mathrm{d}\Delta f(t)}{\mathrm{d}t} = PFR_t + EFR_t - P_L^{max}, \forall t \in \mathcal{T} \tag{2.1}$$

where a positive value for P_L^{max} represents the upper bound for generation loss. Terms PFR_t and EFR_t are the aggregate PFR and EFR reserves, which can be respectively represented as:

$$PFR_t = \sum_{g\in\mathcal{G}} R_{g,t} + \sum_{n\in\mathcal{N}} R_{n,t}, \forall t \in \mathcal{T}, \text{ and} \tag{2.2}$$

$$EFR_t = \sum_{i\in\mathcal{I}} R_{i,t} + \sum_{s\in\mathcal{S}} R_{s,t}, \forall t \in \mathcal{T} \tag{2.3}$$

The contribution to the PFR service can be provided by conventional power plants $g \in \mathcal{G}$ and FNPP $n \in \mathcal{N}$ (which are slower to respond due to their thermo-mechanical properties), while the contribution to the EFR service can be provided by wind generators $i \in \mathcal{I}$ (with fast dynamics). Furthermore, system inertia H_t that is provided by synchronous generators is given by the following equation:

$$H_t = \sum_{g\in\mathcal{G}} H_g \cdot P_g^{max} \cdot n_g^{up} + \sum_{n\in\mathcal{N}} H_n \cdot P_n^{max} \cdot n_n^{up} - H_L \cdot P_L^{max}, \forall t \in \mathcal{T} \tag{2.4}$$

where the system inertia is proportional to the conventional power plant's inertia constant H_g and the rated power P_g^{max}, as well as its

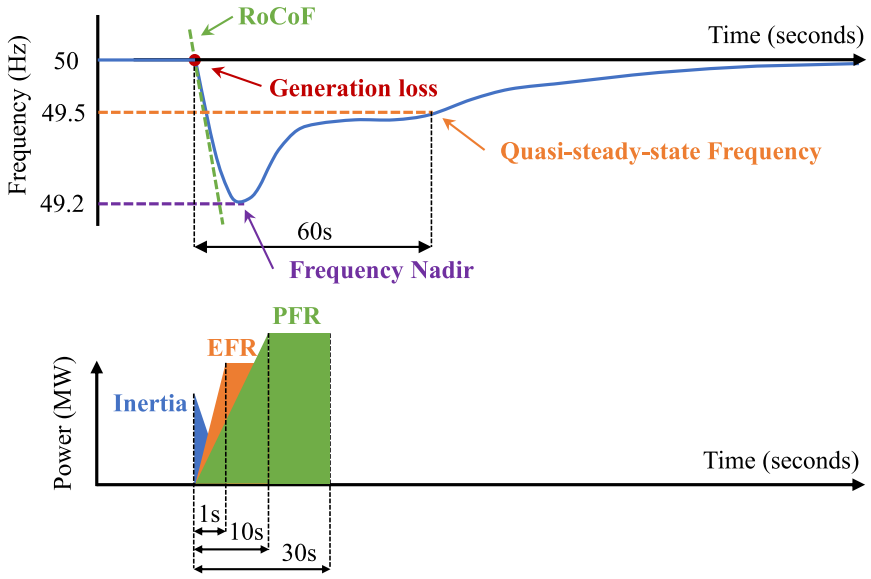

Fig. 2. The three post-fault frequency security requirements that must be met in an event of a generation outage.

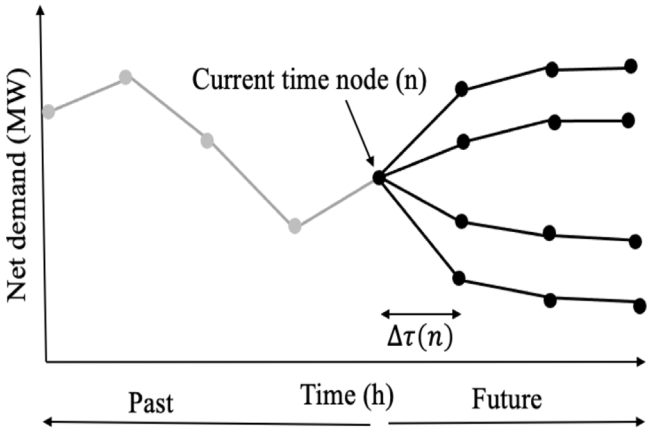

Fig. 3. The schematic for the scenario tree used in the SUC model.

commitment state n_g^{up}. Additionally, the flexible nuclear power plant can be utilised to provide EFR in the system which is proportional to the flexible nuclear power plant's inertia constant H_n and rated power P_n^{max}, and depends on its commitment state n_n^{up}.

3. Mathematical formulation for the proposed optimisation model

This paper aims to investigate the behaviour of FNPP in a frequency security-constrained model that guarantees power system stability at all times. For this research, the AS constraints discussed in Section 2 have been integrated into the SUC model.

3.1. Stochastic unit commitment model

This framework allows for quantifying the benefits of FNPP while explicitly considering the provision of AS in a low-inertia power grid. The formulation of the model presented here assumes branching the scenario tree at the current-time node and branching at each node ahead as shown in Fig. 3. Branching at the current node was not only considered for simplicity but also for significantly reducing computational time [35]. The rolling planning approach considered in the SUC is based on two steps:

1. The whole optimisation is carried out for a 24-hour period in hourly time steps; the current decision in the current time node is considered and applied, while the rest are discarded.
2. In the next time step, the stochastic variables and updated forecasts become available, and then a new scenario tree is built for the next 24 h.

It is worth noting that various techniques have been developed for uncertainty modelling, e.g., Robust Optimisation (RO), Chance-Constrained Programming (CCP), and Stochastic Programming (SP) [10,36]. Overall, RO methods typically address worst-case scenarios, often resulting in conservative decisions, higher operational costs, and reduced efficiency. CCP approaches embed uncertainties into constraints with predefined confidence levels, offering computational efficiency, but can become complex when dealing with multiple or nonlinear constraints. In this context, the proposed SP-based method with an appropriate balance between solution quality and computational time can lead to much more reasonable solutions. In particular, SP-based methods allow decision-makers to evaluate the performance of the suggested decision-making under different situations. In addition, the potential computational burden may be eased by scenario reduction techniques [36].

The objective function of the ASCSUC optimisation model, formulated as MILP, is to minimise the expected operational cost and the emissions cost of all conventional power plants and the expected operational cost of FNPP at each node in the scenario tree (Fig. 3), weighted by the probability of reaching that node, $\pi(n)$:

$$\min \sum \pi(n) \sum (C_g(n) + C_e(n) + C_n(n)) \tag{3.1}$$

The probability $\pi(n)$, associated with node n, is calculated from the user-defined quantiles using the procedure defined in [35]. The following equations give the operational cost and emissions cost of conventional power plants and operational cost for FNPP:

$$C_g = C_g^s n_g^{sg} + \Delta\tau(n)(C_g^{nl} n_g^{up} + C_g^m P_{g,t}), \forall t \in \mathcal{T} \tag{3.2}$$

$$C_e = \lambda^{CO2} \cdot CI_g \cdot P_{g,t}, \forall t \in \mathcal{T} \tag{3.3}$$

$$C_n = C_n^f \cdot h_{sg,t}, \forall t \in \mathcal{T} \tag{3.4}$$

where $\Delta\tau(n)$ is the time interval related to node n, λ^{CO2} is the carbon price for conventional power plants, and CI_g is the carbon intensity of that generator in gCO_2/kWh. C_n^f represents the fuel cost for nuclear

power plant in £/MWh and $h_{sg,t}$ represents the steam generated in the steam generator in MW_{th}.

The generation-demand balance constraint ensures that the system demand is always met by total generation output from conventional power plants, wind turbines, FNPPs and BESS:

$$\sum_{g\in\mathcal{G}} P_{g,t} + \sum_{n\in\mathcal{N}} P_{n,t} + \sum_{i\in I}(P_{i,t} - P^{curt}_{i,t}) + \sum_{s\in S}(P^{d}_{s,t} - P^{c}_{s,t}) = D_t, \forall t \in \mathcal{T} \quad (3.5)$$

3.2. Post-fault frequency security requirements

The three post-fault frequency security requirements described in Section 2.2 are obtained from (2.1) as follows.

RoCoF achieves maximum value at the instant when there is a generation outage in the system. The constraint that guarantees RoCoF security is obtained from solving the swing equation (2.1) at the time of outage ($t = 0$), when frequency deviation is effectively zero and the power contribution from FR is zero:

$$\text{RoCoF}^{max} \geq \frac{P^{max}_{L} \cdot f_0}{2H_t}, \forall t \in \mathcal{T} \quad (3.6)$$

Frequency nadir depends on system inertia and FR. To avoid the activation of LFDD, Nadir must be above the defined threshold which is given by the following equation:

$$\left(\frac{H_t}{f_0} - \frac{EFR_t \cdot T_{EFR}}{4\Delta f_{max}}\right) \cdot \frac{PFR_t}{T_{PFR}} \geq \frac{(P^{max}_{L} - EFR_t)^2}{4\Delta f_{max}}, \forall t \in \mathcal{T} \quad (3.7)$$

where T_{PFR} and T_{EFR} indicate the delivery time of PFR and EFR services, respectively. The detailed formulation for how to obtain Nadir equation (3.7) can be found in [37]. Note that Eq. (3.7) represents a Second-Order Cone (SOC), which can be solved using commercial software such as Gurobi.

Finally, the q-s-s requirement can be obtained from Eq. (2.1) by making RoCoF equal to zero:

$$P^{max}_{L} \leq (EFR_t + PFR_t), \forall t \in \mathcal{T} \quad (3.8)$$

3.3. Flexible nuclear power plant constraints

Modelling individual generators in the SUC model is computationally very costly. The technique of formulating large groups of generators using continuous variables to keep track of aggregated power output for large groups of generators has been proposed in [35]. Therefore, for this research, the proposed ASCSUC model formulates FNPPs and conventional power plants as groups of generators, as shown in [38].

As discussed in Section 2.1, the FNPP consists of PSRC, SSRC, SG and TES. The constraints for power generation output limits for PSRC and SSRC components of the FNPP are formulated as:

$$n^{up}_{n} \cdot P^{min}_{psrc} \leq P_{psrc,t} \leq n^{up}_{n} \cdot P^{max}_{psrc}, \forall t \in \mathcal{T} \quad (3.9)$$

$$n^{up}_{n} \cdot P^{min}_{ssrc} \leq P_{ssrc,t} \leq n^{up}_{n} \cdot P^{max}_{ssrc}, \forall t \in \mathcal{T} \quad (3.10)$$

The aggregate power generation output from an FNPP is the total sum of the power output from PSRC and SSRC formulated as:

$$P_{n,t} = P_{psrc,t} + P_{ssrc,t}, \forall t \in \mathcal{T} \quad (3.11)$$

The provision of FR that each FNPP can provide through its components PSRC and SSRC at time t is constrained by the following constraints:

$$0 \leq R_{psrc,t} \leq R^{max}_{psrc}, \forall t \in \mathcal{T} \quad (3.12)$$

$$R_{psrc,t} \leq n^{up}_{n} \cdot P^{max}_{psrc} - P_{psrc,t}, \forall t \in \mathcal{T} \quad (3.13)$$

$$0 \leq R_{ssrc,t} \leq R^{max}_{ssrc}, \forall t \in \mathcal{T} \quad (3.14)$$

$$R_{ssrc,t} \leq n^{up}_{n} \cdot P^{max}_{ssrc} - P_{ssrc,t}, \forall t \in \mathcal{T} \quad (3.15)$$

Charging and discharging rates of the TES component of the FNPP is limited by the following constraints:

$$0 \leq h^{c}_{tes,t} \leq P^{max}_{tes} \quad (3.16)$$

$$0 \leq h^{d}_{tes,t} \leq P^{max}_{tes} \quad (3.17)$$

The limit on maximum energy that can be stored in the TES of the FNPP is given by the following equation:

$$0 \leq P_{tes,t} \leq P^{max}_{tes} \quad (3.18)$$

The TES energy balance and the limits on its energy content are formulated by the following expression:

$$P_{tes,t} = P_{tes,(t-1)} + \Delta\tau(h^{c}_{tes,t} \cdot \eta^{tes,c} - \frac{h^{d}_{tes,t}}{\eta^{tes,d}}), \forall t \in \mathcal{T} \quad (3.19)$$

The constraint for the heat output of the SG is formulated as follows:

$$h^{min}_{sg} \leq h_{sg,t} \leq h^{max}_{sg}, \forall t \in \mathcal{T} \quad (3.20)$$

Heat balance equations for the whole FNPP take into account the output from the SG, heat consumption of PSRC and SSRC components of the FNPP and also the charging and discharging of the TES units:

$$h_{sg,t} - h^{c}_{tes,t} = nlhr_{psrc} + vhr_{psrc} \cdot P_{psrc,t}, \forall t \in \mathcal{T} \quad (3.21)$$

$$h^{d}_{tes,t} = nlhr_{ssrc} + vhr_{ssrc} \cdot P_{ssrc,t}, \forall t \in \mathcal{T} \quad (3.22)$$

3.4. Conventional power plant constraints

The power generation of a conventional power plant is constrained by:

$$n^{up}_{g} \cdot P^{msg}_{g} \leq P_{g,t} \leq n^{up}_{g} \cdot P^{max}_{g}, \forall t \in \mathcal{T} \quad (3.23)$$

where conventional power plants are part-loaded to provide headroom for FR services. Due to the physical limits of a conventional power plant, the maximum amount that each generator could contribute to provide FR services is limited. The amount of FR that each generator can provide is limited by its maximum response capability (3.24) and the FR provision with the spinning headroom (3.25):

$$P_{g,t} - P_{g,(t-1)} \leq R^{U}_{g}, \forall t \in \mathcal{T} \quad (3.24)$$

$$P_{g,(t-1)} - P_{g,t} \leq R^{D}_{g}, \forall t \in \mathcal{T} \quad (3.25)$$

The provision of FR that each generator can provide at time t is constrained by the following constraints:

$$0 \leq R_{g,t} \leq R^{max}_{g}, \forall t \in \mathcal{T} \quad (3.26)$$

$$R_{g,t} \leq n^{up}_{g} \cdot P^{max}_{g} - P_{g,t}, \forall t \in \mathcal{T} \quad (3.27)$$

3.5. Renewable energy sources constraints

Total power output from inverter-based sources (belonging to subset I) is the aggregate of the power output from wind generation [39].

$$P_{i,t} = P_{wind}, \forall t \in \mathcal{T} \quad (3.28)$$

The provision of FR that wind can provide at time t is modelled by the following constraints:

$$0 \leq R_{i,t} \leq R^{max}_{i}, \forall t \in \mathcal{T} \quad (3.29)$$

$$0 \leq R_{i,t} \leq P^{curt}_{i,t}, \forall t \in \mathcal{T}, \forall t \in \mathcal{T} \quad (3.30)$$

$$0 \leq P_{i,t}^{curt} \leq P_i^{max}, \forall t \in \mathcal{T} \tag{3.31}$$

The FR that can be obtained from wind is then integrated into the optimisation through the frequency security constraints discussed in Section 2.2. The frequency security constraints ensure that the post-fault frequency remains within the defined limits in the event of a major generation outage in the system.

3.6. Battery energy storage constraints

The operational constraints for BESS are given by expressions (3.32)–(3.39). The charging and discharging limits are constrained by (3.32)–(3.35):

$$0 \leq P_{s,t}^{c} \leq P_s^{cmax} : \forall s \in \mathcal{S}, \forall t \in \mathcal{T} \tag{3.32}$$

$$0 \leq P_{s,t}^{c} \leq (1-b) \cdot P_s^{cmax}, \forall s \in \mathcal{S}, \forall t \in \mathcal{T} \tag{3.33}$$

$$0 \leq P_{s,t}^{d} \leq P_s^{dmax} : \forall s \in \mathcal{S}, \forall t \in \mathcal{T} \tag{3.34}$$

$$0 \leq P_{s,t}^{d} \leq b \cdot P_s^{dmax}, \forall s \in \mathcal{S}, \forall t \in \mathcal{T} \tag{3.35}$$

The energy balance constraint for BESS is represented by the following constraints: (3.36)–(3.37) represent the BESS energy balance constraints.

$$E_s^{min} \leq E_{s,t} \leq E_s^{max}, \forall s \in \mathcal{S}, \forall t \in \mathcal{T} \tag{3.36}$$

$$E_{s,t} = E_{s,t-1} + P_{s,t}^{c} \cdot \eta_s^{c} - \frac{P_{s,t}^{d}}{\eta_s^{d}}, \forall s \in \mathcal{S}, \forall t \in \mathcal{T} \tag{3.37}$$

Finally, constraints (3.38)–(3.39) consider the provision of EFR from BESS.

$$0 \leq R_{s,t} \leq R_s^{max}, \forall s \in \mathcal{S}, \forall t \in \mathcal{T} \tag{3.38}$$

$$R_{s,t} \leq P_s^{dmax} - P_{s,t}^{d} + P_{s,t}^{c}, \forall s \in \mathcal{S}, \forall t \in \mathcal{T} \tag{3.39}$$

The FR that can be obtained from BESS is incorporated into the optimisation model through the frequency security constraints detailed in Section 2.2. These constraints ensure that, in the event of a major generation outage, the post-fault system frequency remains within predefined security limits.

3.7. Summary of the mathematical formulation

This subsection summarises the key elements of the proposed mathematical formulation, which underpins a stochastic unit commitment model for co-optimising energy production and AS under uncertainty. Each equation group listed below represents a core aspect of the system operation and optimisation framework:

$$\begin{aligned}
&\min \text{obj. (3.1)} \\
&\textbf{subject to}: \\
&\textit{generation-demand balance}: \text{(3.5)} \\
&\textit{post-fault frequency security}: \text{(3.6)–(3.8)} \\
&\textit{flexible nuclear power plant}: \text{(3.9)–(3.22)} \\
&\text{conventional power plant: (3.23)–(3.27)} \\
&\textit{inverter-based sources}: \text{(3.28)–(3.31)} \\
&\textit{battery energy storage}: \text{(3.32)–(3.39)}
\end{aligned} \tag{3.40}$$

These objective function and constraints form a stochastic unit commitment model that co-optimises energy production and AS under uncertainty. The schematic shown in Fig. 4 provides a visual representation of the proposed SUC model, illustrating the key components, decision variables, system constraints, and their interactions within the optimisation framework. The proposed ASCSUC model co-optimises energy production and AS while ensuring frequency security in low-inertia power systems. It incorporates a scenario-based planning framework that accounts for uncertainties in wind, using a rolling planning approach to update decisions based on the latest forecasts. The model's objective is to minimise the expected total operational and emission costs across all scenarios, subject to a range of operational constraints. These include generation-demand balance, post-fault frequency security requirements (RoCoF, frequency nadir, and quasi-steady-state), and detailed operational limits for conventional generators, inverter-based sources, FNPPs and BESS. The FNPP is modelled with subcomponents—Primary and Secondary Steam Rankine Cycles (PSRC, SSRC), Steam Generator (SG), and Thermal Energy Storage (TES)—to capture its flexibility in both electricity and heat provision. This integrated framework ensures the reliable operation of a decarbonising power system by enabling flexible, low-carbon generation to actively contribute to frequency regulation.

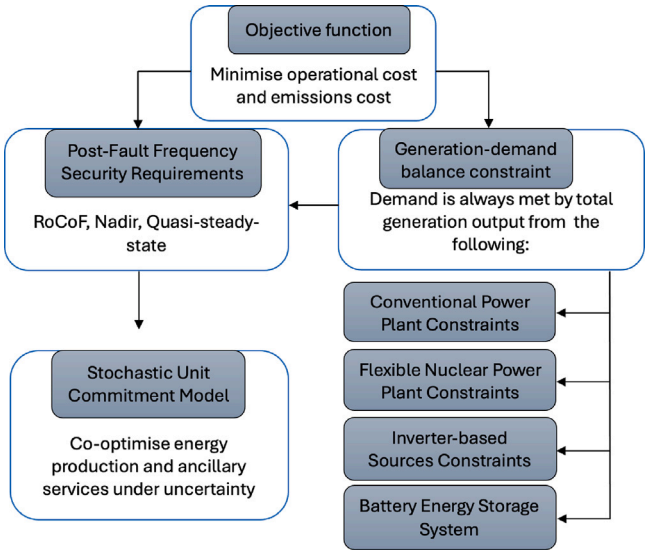

Fig. 4. The visual representation for the proposed model.

4. Case studies

In this section, we evaluate the effectiveness of the ASCSUC model proposed in Section 3, by simulating several case studies for the 2030 GB power system. Each case study was simulated for a 24-hour horizon in half-hourly resolution. Technical characteristics of conventional power plants used in these simulations are taken from [40] and presented in Table 2. The operating cost of conventional power plants is associated with the marginal cost of each generator type. Conversely, the marginal cost of wind generation has been assumed to be zero. A BESS with a total capacity of 5,000 MW, a 2-hour duration, and a 95% roundtrip efficiency is assumed to be connected to the system. Of this capacity, 1,000 MW is allocated specifically for providing Enhanced Frequency Response (EFR) services.

Other parameters considered in the simulations were based on the GB power system regulations: the largest loss $P_t^{Loss} = 1.8$ GW [41], $RoCoF = 1$ Hz/s, $\Delta f_{max} = 0.8$ Hz, the time required for PFR to be delivered is $T_{PFR} = 10$ s and the time required for EFR to be delivered is $T_{EFR} = 1$ sec [31]. The carbon price/tax is selected as 52.56 £/tCO_2 for 2022 [42].

The proposed ASCSUC model is a nonconvex, mixed-integer stochastic optimisation problem, primarily due to unit commitment binary variables and frequency-security constraints. It is NP-hard, with computational complexity increasing exponentially with the number of time

Table 2
Technical parameters of conventional power plants.

Type	Nuclear	CCGT	OCGT
Number of units	6	100	30
Maximum power limit (MW)	1,800	500	100
Min stable generation (MW)	1,799	250	50
Ramp-rate (MW/h)	100	250	50
No-load cost (£/h)	0	4,500	3,000
Start-up cost (£)	N/A	10,000	0
Shut-down cost (£)	N/A	3,000	0
Marginal cost (£/MWh)	10	47	200
Inertia constant (s)	5	4	4
PFR capacity (MW)	0	50	20

periods, units, and wind scenarios. To solve this complex problem, we utilise Gurobi optimisation software [43], a widely-used commercial solver, which allows us to handle large-scale instances efficiently despite the challenges associated with its nonconvex and stochastic nature. The simulations were run using the convex system modelling framework, CVXPY [44], which is an open-source Python-based package for energy system modelling and optimisation.

4.1. Value of optimising FR from flexible nuclear power plant, wind and BESS as a distinct service

In the current GB system operation practice, nuclear power plants and wind are only utilised for energy production and not for the provision of FR services. Therefore, this section explores the importance of co-optimising FR service provision from FNPP, wind and BESS as proposed in Section 3, by demonstrating cost savings under both low and high wind scenarios (corresponding to 30 GW and 60 GW of installed wind capacity). In order to quantify the benefits of co-optimising FR services from FNPP, wind and BESS, compared to the counterfactual when no FR is provided from any of the three technologies, several case studies were conducted. Five different operating strategies have been considered for the analysis using the model proposed in Section 3:

1. PFR provided only by conventional power plants (base case): EFR is not defined as a distinct service, given that in the current GB grid operation, the RES and nuclear power plant are utilised only for energy production and not for FR provision.
2. Optimised EFR from wind (Wind): EFR provision from wind is optimised as a distinct service.
3. Optimised PFR from FNPP (FNPP): PFR provision from FNPP is optimised as a distinct service.
4. Optimised EFR from BESS (BESS): EFR provision from BESS is optimised as a distinct service.
5. Full optimisation (full-opt): the model optimises EFR provision from wind and PFR provision from FNPP; the latter is co-optimised as a distinct service along with PFR and inertia from conventional power plants.

Fig. 5 illustrates the system operation cost savings obtained from "Wind", "FNPP", "BESS" and "full-opt" cases, with respect to the "base case" strategy. As expected, all four operating strategies "Wind", "FNPP", "BESS" and "full-opt" demonstrate system cost savings when compared to the "base case". The results suggest that in all cases the system cost savings were significantly higher in the high wind scenario than in the low wind scenario. In both low and high wind scenarios the cost savings are observed to be the highest under the "full-opt" strategy, when compared to the "Wind", "FNPP" and "BESS" strategies. This is driven by the fact that full optimisation of FR provision in the high wind scenario significantly reduces the amount of energy required from conventional power plants, resulting in a significantly reduced amount of inertia in the system, resulting in a further increase in the volume of required FR services. In this situation, the provision of PFR from FNPP

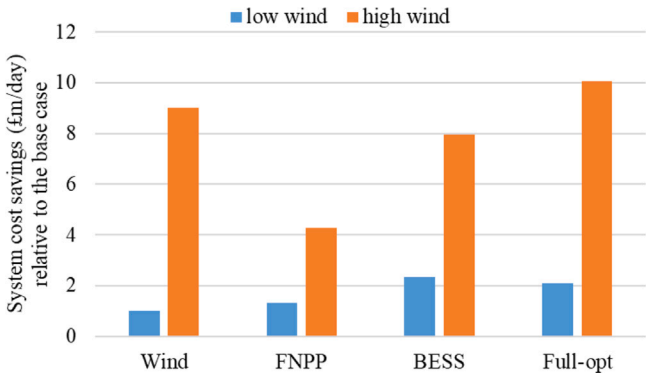

Fig. 5. System cost savings under different scheduling methods for two different levels of wind in the system.

and EFR from wind and BESS can reduce the volume of AS provided from conventional power plants, which results in fewer conventional power plants operating and therefore reduces system operation cost.

Furthermore, the results demonstrate that the cost savings in the low wind scenario are higher for the "FNPP" strategy than for the "Wind" strategy, suggesting very significant system benefits from optimising flexibility from the nuclear power plant. On the other hand, the system cost savings in the high wind scenario are higher in the "Wind" and "BESS" case than in the "FNPP" case. This emphasises the benefits of optimising EFR, which, due to the faster provision, represents a more valuable service for the grid than PFR. Provision of EFR from wind or BESS, especially in the high wind scenario, can significantly reduce the requirement for PFR service from conventional power plants to meet the nadir constraint.

The computation times for the five simulation cases are summarised as follows. The base case, involving only conventional PFR provision, required approximately 224 s to complete. The "Wind" case, where EFR is optimally scheduled from wind resources, took about 397 s. The "FNPP" and "BESS" cases, with optimal PFR provision from FNPPs and EFR provision from BESS, had a similar computational demand, requiring around 440 s. The most computationally intensive configuration, the "full-opt" case, which involves joint optimisation of both EFR from wind and PFR from FNPP, required approximately 530 s to complete. As expected, the full co-optimisation model has a higher computational burden due to the increased dimensionality and scenario complexity from the quantile-based scenario tree approach. Nevertheless, the additional computation time is justified by the improved system cost savings observed.

To further analyse the computational complexity of the proposed ASCSUC model, a detailed comparison of computing times is conducted across three cases: (1) a deterministic model (DS) without any uncertainties, (2) a stochastic model (SS-1) considering 5 scenarios with different probabilities, and (3) a stochastic model (SS-2) considering 10 scenarios with different probabilities. As indicated in Table 3, the deterministic model requires 24.86 s to converge, while the two stochastic models (SS-1 and SS-2) impose significantly higher computational burdens, requiring 354.2 s and 1075 s, respectively, to reach convergence. This increase in computational time is attributed to the larger number of decision variables and constraints introduced by the additional scenarios, as summarised in Table 3. The results highlight a fundamental trade-off in scenario-based stochastic optimisation: increasing the number of scenarios improves the model's robustness to uncertainty, while significantly increasing the solution time. This might become particularly critical for large-scale power systems or real-time applications, where computational efficiency is essential. Therefore, more advanced scenario selection and reduction techniques could be considered in future work to balance accuracy and computational feasibility. In addition, solver performance and hardware specifications can

Table 3
Comparison of computational complexity among a deterministic model and two stochastic models.

	DS	SS-1	SS-2
Computing time (s)	24.86	354.2	1075
Variables	14160	57936	101712
Constraints	21340	106696	192052

further influence total runtime, suggesting the potential benefit of parallel computing or decomposition methods for scalability. Furthermore, more advanced approaches for uncertainties, such as distributional robust optimisation, model-free learning algorithms, and even end-to-end learning methods, should be developed to handle the potential computational issues in real-world applications.

4.2. Impact of co-optimising FR from flexible nuclear power plant, wind and BESS on RES utilisation

One of the key research challenges addressed in this work is the co-optimisation of FNPP in a frequency security-constrained optimisation framework while considering the uncertainty from RES, with the aim of enhancing RES utilisation. This section, therefore, studies the impact of co-optimising the FR from FNPP, wind and BESS on RES curtailment. The same five cases were considered here as discussed in Section 4.1, and compared for both low and high wind scenarios.

The results in Fig. 6 demonstrate that co-optimising FR from FNPP, wind and BESS can reduce wind curtailment in both low and high wind scenarios. As expected, in the low wind scenario, the wind curtailment is lower due to the lower absolute level of wind output. Also, wind curtailment is lower for the "FNPP" strategy than for the "Wind" and "BESS" strategies, because when there is no EFR in the system, inertia and PFR requirement from conventional power plants and FNPP increase to comply with the nadir requirement. This results in more conventional power plants being online as well as the utilisation of PFR from FNPP, which leads to reduced power output from FNPP. This, in turn, allows more wind output to be utilised and less of it to be curtailed.

On the other hand, in the high wind scenario, the wind curtailment is higher for the "FNPP" strategy than for the "Wind" and "BESS" strategies. This can be explained by the high level of wind output and optimised EFR provision from wind and BESS, which significantly reduces the requirement for PFR from conventional power plants and requires fewer of them to be online and produce electricity at least at the minimum output level. This will result in better wind utilisation. On the other hand, when only FNPP is optimised, the PFR requirement is relatively high, so more conventional units are brought online and the power generation from FNPP is optimised to provide PFR, leaving less room for wind utilisation and causing higher wind curtailment.

The highest cost savings observed for the "full-opt" strategy when co-optimising PFR from FNPP and EFR from wind are driven by two main factors: the "full-opt" strategy reduces the number of synchronised conventional units that also need to provide energy, and therefore allows more wind output to be utilised and reduces curtailment; also, the "full-opt" strategy reduces the requirement for FR to be provided by conventional generators. These two aspects can be illustrated by presenting the detailed hourly power supply in the GB power system.

Results in Fig. 7 present the hourly supply–demand balance in the GB power system for the low-wind scenario. The results show that during the first 6 h of the day and in hours 21 to 24, when the demand is low, wind curtailment is relatively high in the base case. On the other hand, co-optimising FR from FNPP and wind using the proposed ASCSUC model can unlock additional flexibility and hence reduce RES curtailment. Finally, the results in Fig. 8 illustrate that in the high-wind scenario, there is wind curtailment during most hours of the day in the "base case", as well as in the "full-opt" strategy. Curtailment

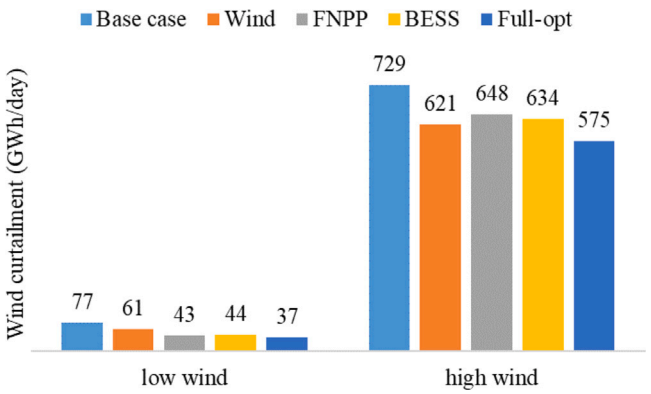

Fig. 6. Impact of co-optimising PFR from FNPP and EFR from wind on wind output curtailment.

reduces in the "full-opt" case because co-optimising FR from FNPP and wind allows for flexible variations in their output and for FR services provision, hence resulting in improved RES utilisation.

4.3. Impact of co-optimising FR from FNPP, wind and BESS on emission cost

System integration of low-carbon generation raises several challenges, some of which have been addressed in this paper. The technical aspect of the challenge is associated with the variable nature of RES and the absence of inherent inertia, which increases the need for AS provision to ensure system security. The economic aspect of the challenge is associated with limited load-following capabilities of nuclear power plants, which increases the volume of AS that needs to be sourced from conventional power plants, and therefore increases the cost and carbon emissions associated with providing AS. This subsection aims at investigating the benefits of co-optimising FR provision from FNPP, wind and BESS not only for providing frequency security but also for reducing emission costs.

A detailed analysis was conducted using the five strategies introduced in Section 3.1 under two levels of wind low and high wind scenarios. Results in Fig. 9 show that co-optimising FNPP and EFR from wind in the "full-opt" strategy can reduce emissions cost when compared to the other three cases, indicating the value of simultaneous co-optimisation of FNPP and EFR from wind as a distinct service. Co-optimising FNPP and EFR from wind reduces the number of conventional units that need to be in synchronous operation, which results in lower inertia provided by conventional power plants. Declining system inertia from conventional generators makes FNPP and EFR from wind more valuable, as they reduce the requirement for energy and AS to be provided from conventional power plants. This in turn results in a decreased amount of fuel required to generate electricity from conventional generators and hence reduced carbon emissions. This phenomenon can be further understood by studying the operation of the individual components of the FNPP. For this purpose, a detailed analysis of the individual components of FNPP has been conducted.

Furthermore, a sensitivity analysis was conducted to evaluate the impact of varying carbon price intensities on system emissions cost. Specifically, three distinct cases were considered: Case 1 representing a low carbon price intensity, Case 2 with a medium carbon price, and Case 3 with a high carbon price scenario. These cases were selected to reflect a range of plausible future policy and market conditions. The results in Fig. 10 show that under Case 1, conventional power plants remain economically attractive due to the relatively low penalty for carbon emissions. However, as carbon pricing increases in Cases 2 and 3, the cost of relying on high-emission generation rises significantly. In Case 3, with high carbon pricing, the system clearly favours the

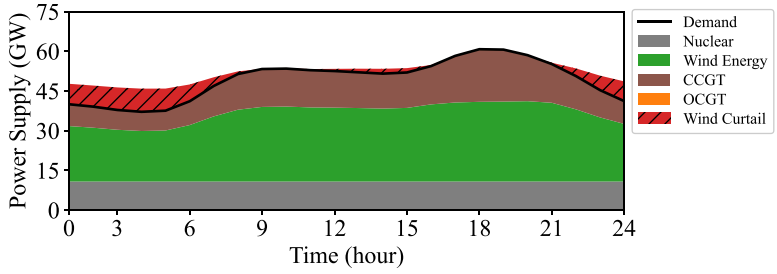

(a) Base case

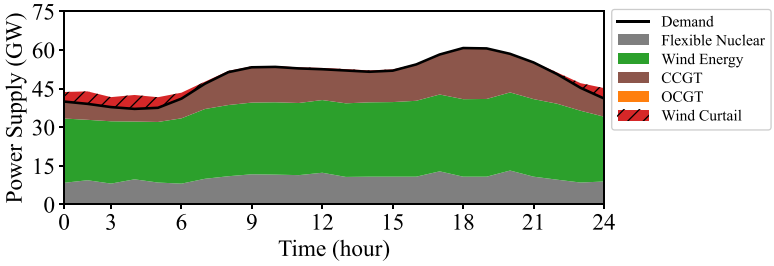

(b) Full-opt

Fig. 7. Hourly power supply in the GB power system for the low-wind scenario, for base case (a) and Full-opt (b) strategies.

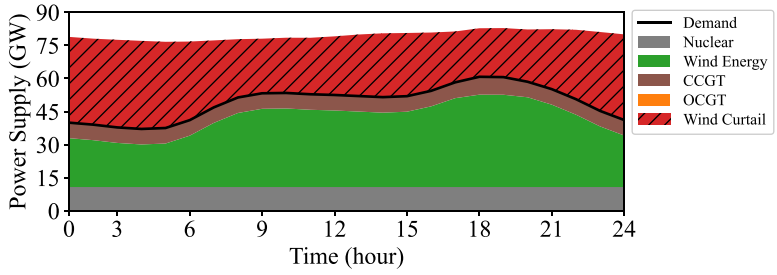

(a) Base case

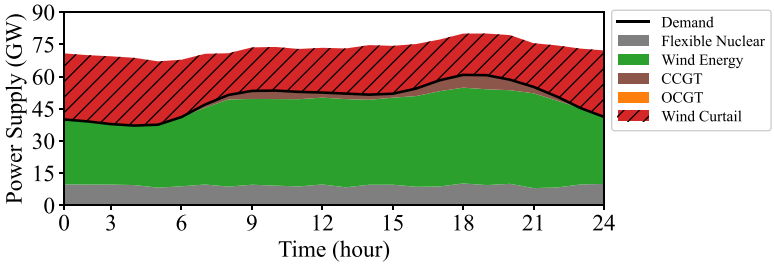

(b) Full-opt

Fig. 8. Hourly power supply in the GB power system for the high-wind scenario, for base case (a) and Full-opt (b) strategies.

co-optimisation of FNPPs, wind, and BESS, which provide frequency response and system flexibility with minimal emissions. This shift results in a substantial reduction in emissions costs and decreased dependence on conventional power plants. The analysis demonstrates the importance of incorporating carbon pricing into long-term power system planning, as it strongly influences the economic competitiveness of low-carbon technologies and reinforces the value of co-optimised flexibility strategies under increasingly stringent climate policies.

Fig. 11 presents the daily operation of FNPP components for the "base case" and "full-opt" strategies. The results illustrate that in hours 9 to 21, when demand is at its peak, as evident from Fig. 8, the power output of the PSRC increases. When considering the power output of SSRC, it can be observed that during the peak demand hours, i.e., hours 9 to 12 and 18 to 21, the power output of SSRC increases to supply additional energy to the system. This lowers the requirement for electricity output from other sources, such as conventional power plants. The results also show an increase in SG output during high-demand periods.

In addition, the results in Fig. 11 show that during peak demand hours, when the power output from SSRC increases, there is a reduction in the energy stored in TES; this highlights the benefits that the TES component of FNPP can provide by enabling additional supply at the

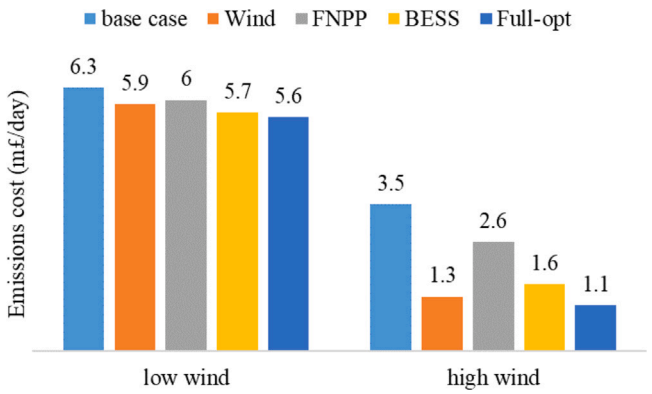

Fig. 9. Carbon emissions cost obtained from five different strategies under low and high wind scenarios.

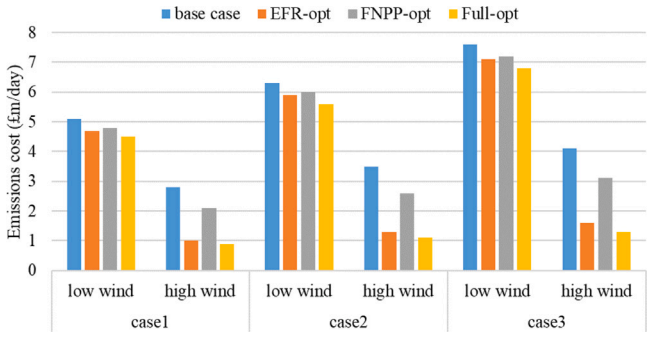

Fig. 10. Carbon emissions cost obtained under three different carbon price cases.

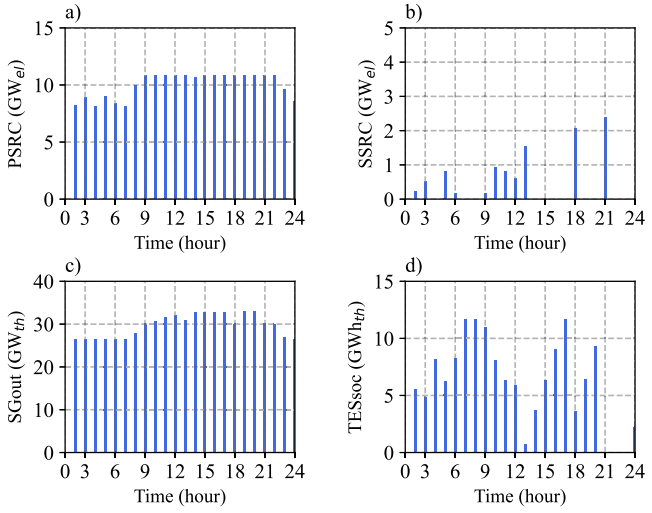

Fig. 11. Hourly operation of the components of flexible nuclear power plant under low wind scenario; (a) PSRC, (b) SSRC, (c) SG; and (d) TES.

time of need. During low net demand periods (demand minus RES output), the amount of power generated by the PSRC reduces, and the excess steam from SG is utilised to charge TES. The energy from TES can then later be used to operate SSRC and generate additional output during high-demand periods.

4.4. Benefit of full-optimisation on frequency services cost under different wind scenarios

The final part of the analysis focuses on co-optimising FR services from FNPP, wind and BESS to assess the cost of providing FR services

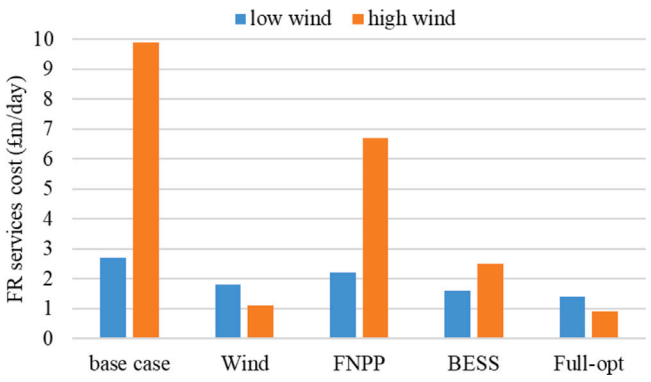

Fig. 12. Cost of FR services when considering FNPP and EFR from wind under different levels of wind.

under various wind scenarios. In this analysis the cost of FR services has been quantified as the difference between the total system operating cost with and without considering the FR requirements represented in Eq. (3.7). Most of the FR needed to comply with the frequency security constraints is typically provided by operating part-loaded conventional power plants. Running a high number of part-loaded generators is more expensive than producing the same amount of energy from a lower number of fully-loaded generators, and can cause wind curtailment. The results in Fig. 12 presents the impact of co-optimising PFR from FNPP and EFR from wind and BESS on the cost of providing FR services. The results show that for "base case" and "FNPP", the FR service cost is higher in the high wind scenario than for low wind, as high wind output means fewer conventional plants are required to produce energy. However, to provide system security, many more part-loaded conventional generators need to be brought online to provide FR services, which consequently increases the FR cost.

It can be observed that all optimised cases result in lower FR service cost than the "base case", with the "full-opt" strategy resulting in the lowest cost of FR services. This occurs because in the "full-opt" case, when FR services are added into the model, the number of additional conventional units that need to be synchronised to meet the FR requirement is the lowest, as a large part of the requirement is already met by wind generators and FNPP units. As a result, a decrease in FR services cost is observed. Finally, the results demonstrate that the availability of EFR provided by wind generators in a high-wind scenario has the largest effect on reducing the cost of FR provision, given that the speed of EFR delivery effectively makes it a more valuable service than PFR.

5. Conclusions

This paper proposes an ancillary service constrained stochastic unit commitment model that co-optimises the operation of flexible nuclear power plants within a wider power system, accounting for uncertainty from wind. The model schedules energy production alongside various frequency services, including inertia, primary frequency response, and enhanced frequency response. Extensive case studies highlight the benefits of jointly optimising nuclear flexibility and enhanced frequency response provision from wind and battery storage. The proposed approach reduces overall system operation costs and associated carbon emissions. Results demonstrate that co-optimisation increases the flexibility of flexible nuclear power plants, thereby decreasing reliance on conventional synchronised generation to meet energy and frequency response requirements. This leads to lower carbon emissions, reduced operational costs, and improved wind integration through decreased curtailment. These findings have important practical implications for industry stakeholders and policymakers. For system operators and energy planners, the model offers a pathway to enhance grid flexibility

and resilience while facilitating higher renewable penetration. For policymakers, the results support the development of market structures and regulatory frameworks that incentivise flexible nuclear operations and reward the provision of ancillary services, ultimately contributing to more sustainable and cost-effective energy systems. However, the SUC modelling technique used in this research is indeed well-suited for the day-ahead market, particularly for scheduling energy and frequency reserves. However, it inherently does not incorporate real-time adjustments or market mechanisms, which might limit its practical applicability in dynamic operational environments. Therefore, future work should place greater emphasis on developing real-time models, leveraging data-driven methods could be a promising approach to capture the complexities of real-time market operations and system control.

Furthermore, to facilitate the real-world deployment of FNPPs, several non-technical barriers should also be considered alongside the above technological discussions. First, dedicated funding mechanisms, such as public–private partnerships, green financing tools, or government-backed loan guarantees, may lower the high upfront capital costs of FNPPs and reduce investor risk. Second, targeted policy incentives, including tax credits, feed-in tariffs, or carbon pricing mechanisms, may be helpful to improve the economic competitiveness of FNPPs relative to other conventional generation technologies. Third, regulatory frameworks also need to evolve to recognise the unique role of FNPPs in future power systems. Their flexible operation across baseload and load-following modes may require updated licensing procedures, further guidelines on safety protocols and performance standards, and integration into long-term energy planning models. Furthermore, policy alignment at national and regional levels can ensure that FNPPs are included in grid modernisation and clean energy transition strategies. By integrating these economic and policy strategies with advanced engineering solutions, the pathway to scalable and sustainable FNPP deployment may be significantly accelerated.

Finally, in future work, it will be interesting to extend this study to power systems in different regions (e.g., the US and EU) that face varying frequency security challenges, by collecting detailed operational data and generation mix information. This will enable a more comprehensive comparison of FNPP performance under diverse grid conditions, regulatory frameworks, and technology portfolios, thereby further validating the model's applicability and informing region-specific planning and policy decisions.

CRediT authorship contribution statement

Aimon Mirza Baig: Writing – review & editing, Writing – original draft, Visualization, Validation, Software, Methodology, Investigation, Formal analysis, Data curation, Conceptualization. **Yi Wang:** Writing – review & editing, Validation, Software, Methodology, Formal analysis, Data curation. **Marko Aunedi:** Writing – review & editing, Validation, Methodology, Data curation. **Goran Strbac:** Writing – review & editing, Supervision, Resources, Project administration, Funding acquisition.

Declaration of competing interest

The authors declare the following financial interests/personal relationships which may be considered as potential competing interests: Aimon Mirza Baig reports financial support was provided by IDLES PROJECT (EDF Energy). If there are other authors, they declare that they have no known competing financial interests or personal relationships that could have appeared to influence the work reported in this paper.

Acknowledgments

This work was supported by the UK EPSRC project: 'Integrated Development of Low-Carbon Energy Systems (IDLES): A Whole-System Paradigm for Creating a National Strategy' (project code: EP/R045518/1).

Data availability

No data was used for the research described in the article.

References

[1] Department for Energy Security & Net Zero. Net zero innovation portfolio and the advanced nuclear fund. 2022.
[2] Department of Business, Energy & Industrial Strategy, Nuclear Industrial Strategy. The UK's nuclear future. 2013.
[3] Denholm P, King JC, Kutcher CF, Wilson PP. Decarbonizing the electric sector: Combining renewable and nuclear energy using thermal storage. Energy Policy 2012;44.
[4] Shakoor A, Davies G, Strbac G, Pudjianto D, Teng F, Papadaskalopoulos D, et al. Roadmap for flexibility services to 2030. 2017.
[5] Al Kindi AA, Aunedi M, Pantaleo AM, Strbac G, Markides CN. Thermo-economic assessment of flexible nuclear power plants in future low-carbon electricity systems: Role of thermal energy storage. Energy Convers Manage 2022;258.
[6] Park JH, Heo JY, Lee JI. Techno-economic study of nuclear integrated liquid air energy storage system. Energy Convers Manage 2022;251.
[7] Strbac G, Pudjianto D, Aunedi M, Papadaskalopoulos D, Djapic P, Ye Y, et al. Cost-effective decarbonization in a decentralized market: The benefits of using flexible technologies and resources. IEEE Power Energy Mag 2019;17(2):25–36.
[8] Loisel R. Power system flexibility with electricity storage technologies: A technical–economic assessment of a large-scale storage facility . Int J Electr Power Energy Syst 2012;42(1):542–52.
[9] Peter C, Vrettos E, Büchi FN. Polymer electrolyte membrane electrolyzer and fuel cell system characterization for power system frequency control. Int J Electr Power Energy Syst 2022;141:108121.
[10] Badesa L, Teng F, Strbac G. Simultaneous scheduling of multiple frequency services in stochastic unit commitment. IEEE Trans Power Syst 2019;34(5):3858–68.
[11] Baig AM, Badesa L, Wang Y, Strbac G. Co-optimising frequency-containment services from zero-carbon sources in electricity grids dominated by renewable. Int J Electr Power Energy Syst 2025;164:110375.
[12] O'Malley C, Badesa L, Teng F, Strbac G. Frequency response from aggregated V2G chargers with uncertain EV connections. IEEE Trans Power Syst 2023;38(4):3543–56.
[13] Chu Z, Markovic U, Hug G, Teng F. Towards optimal system scheduling with synthetic inertia provision from wind turbines. IEEE Trans Power Syst 2020;35(5):4056–66.
[14] International Atomic Energy Agency. Nuclear power for the 21st century: Flexible operation of nuclear power plants. 2018.
[15] Grid N. Future energy scenarios. 2018.
[16] Nuclear Energy Agency. Flexible nuclear energy for clean energy systems. 2022.
[17] International Renewable Energy Agency. Green hydrogen: A guide to policy making. 2020.
[18] Carlson F, Davidson JH, Tran N, Stein A. Model of the impact of use of thermal energy storage on operation of a nuclear power plant rankine cycle. Energy Convers Manage 2019;181.
[19] Duan L, Petroski RW, Caldeira L, Ken. Stylized least-cost analysis of flexible nuclear power in deeply decarbonized electricity systems considering wind and solar resources worldwide. Nat Energy 2022;7.
[20] K B, A W, S S, MS G, M. E. Increasing revenues of nuclear power plants with thermal storage. J Energy Resour Technol Trans ASME 2020;142.
[21] Carlson F, Davidson JH. Parametric study of thermodynamic and cost performance of thermal energy storage coupled with nuclear power. Energy Convers Manage 2021;236.
[22] Li Y, Cao H, Wang S, Jin Y, Li D, Wang X, et al. Load shifting of nuclear power plants using cryogenic energy storage technology. Appl Energy 2014;113.
[23] Carlson F, Davidson JH. Nuclear power coupled with thermal energy storage: Impact of technical performance on economics in an exemplary electricity grid. ASME Open J Eng 2022.
[24] Romanos P, Al Kindi AA, Pantaleo AM, Markides CN. Flexible nuclear plants with thermal energy storage and secondary power cycles: Virtual power plant integration in a UK energy system case study. E Prime Adv Electr Eng Electron Energy 2022;2.
[25] Aunedi M, Al Kindi AA, Pantaleo AM, Markides CN, Strbac G. System-driven design of flexible nuclear power plant configurations with thermal energy storage. Energy Convers Manage 2023;291.
[26] Fernández-Arias P, Vergara D, Orosa JA. A global review of PWR nuclear power plants. Appl Sci 2020;10(13):4434.
[27] Rämä M, Leurent M, Devezeaux de Lavergne J-G. Flexible nuclear co-generation plant combined with district heating and a large-scale heat storage. Energy 2020;193. http://dx.doi.org/10.1016/j.energy.2019.116728.
[28] Moustafa N, Rhodes A, Owen MW. The future of nuclear power in the UK. 2024.
[29] Badesa L, Strbac G, Magill M, Stojkovska B. Ancillary services in great britain during the COVID-19 lockdown: A glimpse of the carbon-free future. Appl Energy 2021;285:116500.

[30] Qiu D, Baig AM, Wang Y, Wang L, Jiang C, Strbac G. Market design for ancillary service provisions of inertia and frequency response via virtual power plants: A non-convex bi-level optimisation approach. Appl Energy 2024;361.
[31] National Grid. Future requirements for balancing services. 2016.
[32] Grid N. System needs and product strategy. 2017.
[33] Badesa L, Teng F, Strbac G. Pricing inertia and frequency response with diverse dynamics in a mixed-integer second-order cone programming formulation. Appl Energy 2020;260:114334.
[34] Kimbark EW. Power system stability. 1, John Wiley & Sons; 1995.
[35] Sturt A, Strbac G. Efficient stochastic scheduling for simulation of wind-integrated power systems. IEEE Trans Power Syst 2012;27(1):323–34.
[36] Wang Y, Rousis AO, Strbac G. A three-level planning model for optimal sizing of networked microgrids considering a trade-off between resilience and cost. IEEE Trans Power Syst 2021;36(6):5657–69.
[37] Badesa L, Matamala C, Zhou Y, Strbac G. Assigning shadow prices to synthetic inertia and frequency response reserves from renewable energy sources. IEEE Trans Sustain Energy 2023;14(1):12–26.
[38] Teng F, Trovato V, Strbac G. Stochastic scheduling with inertia-dependent fast frequency response requirements. IEEE Trans Power Syst 2016;31(2):1557–66.
[39] Teng F, Strbac G. Assessment of the role and value of frequency response support from wind plants. IEEE Trans Sustain Energy 2016;7(2):586–95.
[40] Badesa L, Teng F, Strbac G. Conditions for regional frequency stability in power system scheduling—Part II: Application to unit commitment. IEEE Trans Power Syst 2021;36(6):5567–77.
[41] Department for Business, Energy & Industrial Strategy. Hinkley point c. 2017.
[42] Department for Energy Security and Net Zero. Determinations of the UK ETS carbon price. 2022, URL https://www.gov.uk/government/publications/determinations-of-the-uk-ets-carbon-price.
[43] Anand R, Aggarwal D, Kumar V. A comparative analysis of optimization solvers. J Stat Manag Syst 2017;20(4):623–35.
[44] Diamond S, Boyd S. CVXPY: A python-embedded modeling language for convex optimization. J Mach Learn Res 2016;17(83):1–5.